



ORIGINAL ARTICLE

# A cementless, proximally fixed anatomic femoral stem induces high micromotion with nontraumatic femoral avascular necrosis: A finite element study



Wen-Chuan Chen <sup>a</sup>, Yu-Shu Lai <sup>a,\*</sup>, Cheng-Kung Cheng <sup>a,b</sup>,  
Ting-Kuo Chang <sup>c</sup>

<sup>a</sup> Orthopaedic Device Research Centre, National Yang Ming University, Taipei, Taiwan

<sup>b</sup> Institute of Biomedical Engineering, National Yang Ming University, Taipei, Taiwan

<sup>c</sup> Department of Orthopaedics, Mackay Memorial Hospital, New Taipei City, Taiwan

Received 19 August 2013; received in revised form 4 March 2014; accepted 10 March 2014

Available online 2 April 2014

## KEYWORDS

Femoral head  
necrosis;  
Finite element  
analysis;  
Total hip replacement

**Summary** Decrease in bone mineral density of metaphysis in patients with nontraumatic avascular necrosis of the femoral head (AVN) is considered the main factor leading to aseptic loosening of the femoral component. Researchers have hypothesized that a cementless, anatomic stem fixed proximally to the metaphysis has a higher risk for aseptic loosening than a straight stem that is fixed at the diaphysis in patients with nontraumatic AVN. The purpose of the current study was to evaluate the effects of cancellous bone stiffness at the metaphysis and stem geometry on the micromotion of the femoral stem relative to the femur. The VerSys (straight) and ABG (anatomic) femoral stems were enrolled in this finite element study to determine the performance of prosthetic micromotion. The simulated load to the hip joint during heel strike was assigned. Results showed that the VerSys model represented better resistance in micromotion between the bone/stem interface than the ABG model in either normal or poor cancellous bone stiffness at the metaphysis. The bone quality at the metaphysis of patients with nontraumatic AVN should be considered prior to selecting a femoral stem. In consideration of initial stability, a cementless, straight stem that fits the isthmus is more favourable than an anatomic stem that is fixed to the proximal area of the canal.

Copyright © 2014, The Authors. Published by Elsevier (Singapore) Pte Ltd. This is an open access article under the CC BY-NC-ND license (<http://creativecommons.org/licenses/by-nc-nd/4.0/>).

\* Corresponding author. Orthopaedic Device Research Centre, National Yang Ming University, Number 155, Section 2, Linong Street, Shih-Pai, Beitou District, Taipei 11221, Taiwan. Tel.: +886 2 2826 7355; fax: +886 2 2822 8557.

E-mail addresses: [uesu@mail2000.com.tw](mailto:uesu@mail2000.com.tw), [uesu@ortho.ym.edu.tw](mailto:uesu@ortho.ym.edu.tw) (Y.-S. Lai).

## Introduction

Nontraumatic avascular necrosis of the femoral head (AVN) is the main indication for total hip replacement in young Chinese patients [1,2]. People with a history of alcohol abuse [3] or overdose of cortisone were predisposed to nontraumatic AVN [4,5]. Although patients with nontraumatic AVN are mostly under 50 years of age, a higher prevalence of revision after total hip replacement (THR) than traumatic AVN patients was reported [6,7]. Radl et al. [7] considered that the results might be related to abnormal bone quality, which probably is accelerated by higher mechanical demand in the younger population. Arlot et al. [8] found that there was a significant reduction in trabecular bone volume, thickness of osteoid seams, and rate of calcification in aseptic osteonecrosis patients. Clinical studies found the correlation that poor bone quality at the metaphysis of nontraumatic AVN patients would result in a higher revision rate after THR. To our knowledge, no prior study has evaluated the mechanical effect of femoral stem geometry on nontraumatic AVN patients.

For the design of a femoral stem, the main rationales in stem geometry can be classified into two types: straight and anatomic. The design of a straight stem requires the machined femoral canal to accommodate the stem that fits the isthmus of the femur, whereas the anatomic design is that the prosthesis conforms with the anatomical curvature of the proximal area of the femur [9]. The proximally fixed anatomic stem may be unstable when the bone quality of the metaphysis is poor. The micromotion between stem/bone interfaces inhibited bone ingrowth when the micromotion exceeded  $150\ \mu\text{m}$  [10,11]. We hypothesized that a cementless, anatomic stem has a higher risk for aseptic loosening than a straight stem in patients with nontraumatic AVN. The purpose of this study was to evaluate the effects of metaphysis strength and stem geometry on

the micromotion of a femoral stem relative to the femur by finite element analysis.

## Materials and methods

The finite element model of the femur developed in our previous study [12] was utilized for analyzing the cemented femoral stem. Three-dimensional models of cementless femoral stems—size no. 15 VerSys [straight femoral stem ( $N_S$ ) model; Zimmer Inc., Warsaw, IN, USA] and size number 7 ABG [anatomic femoral stem ( $N_A$ ) model; Howmedica, Allendale, NJ, USA]—were enrolled in this study (Fig. 1). Implantation of femoral stems was manipulated by SolidWorks 2008 (SolidWorks Corp., Concord, MA, USA) until a presumably adequate fit was obtained. The insertion positions of both models were confirmed by a senior surgeon. In order to exclude the effect of a moment arm, which is caused by different neck lengths and neck angles in the two models, the neck length of the stem in the  $N_A$  model was shortened so that the moment arm of the stems in the  $N_S$  and  $N_A$  models were identical. Referring to the consequences of convergence tests, the element numbers for the models were assigned as 68,311 ( $N_S$  model) and 71,457 ( $N_A$  model) with 20-node tetrahedron elements (Fig. 2).

The elastic moduli for stem, femoral cortex, and cancellous bone were 110,000 MPa, 17,000 MPa, and 1500 MPa, respectively, while Poisson's ratio was assigned as 0.3 [13]. The reduction of bone mineral density for cancellous bone at different AVN stages was simulated by decreasing the elastic modulus of cancellous bone from 100% (1500 MPa) to 50% (750 MPa) in 10% decrements. The loading condition was considered to be presented by the heel strike of the gait cycle, which consisted of the loads at the femoral head [4.5 times the body weight with force components:  $(x, y, z) = (1492, 915, -2925)$  N] and the abduction muscle force at the great trochanter [3.45 times

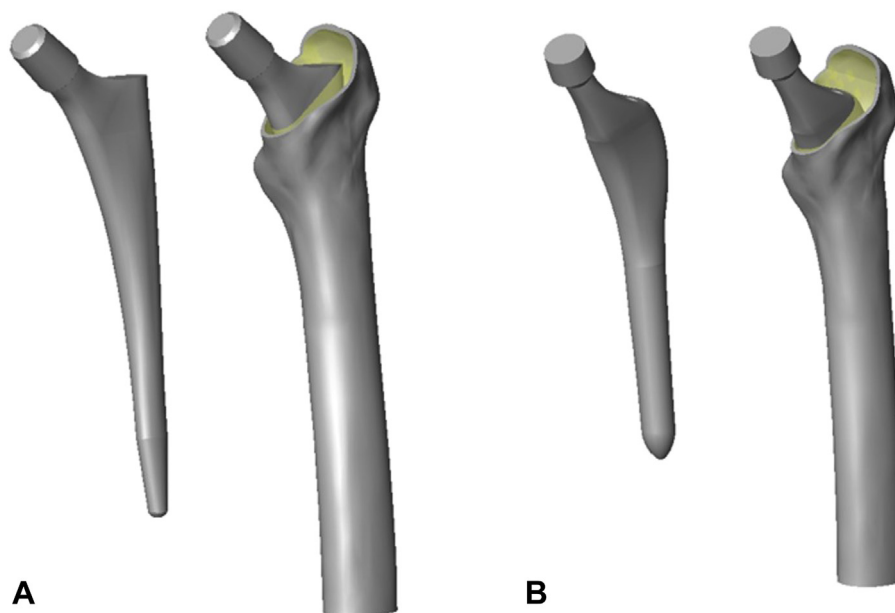


**Figure 1** (A) The  $N_S$  model: a straight, cementless VerSys hip prosthesis. (B) The  $N_A$  model: an anatomic, cementless ABG hip prosthesis implanted in a validated femoral bone model.

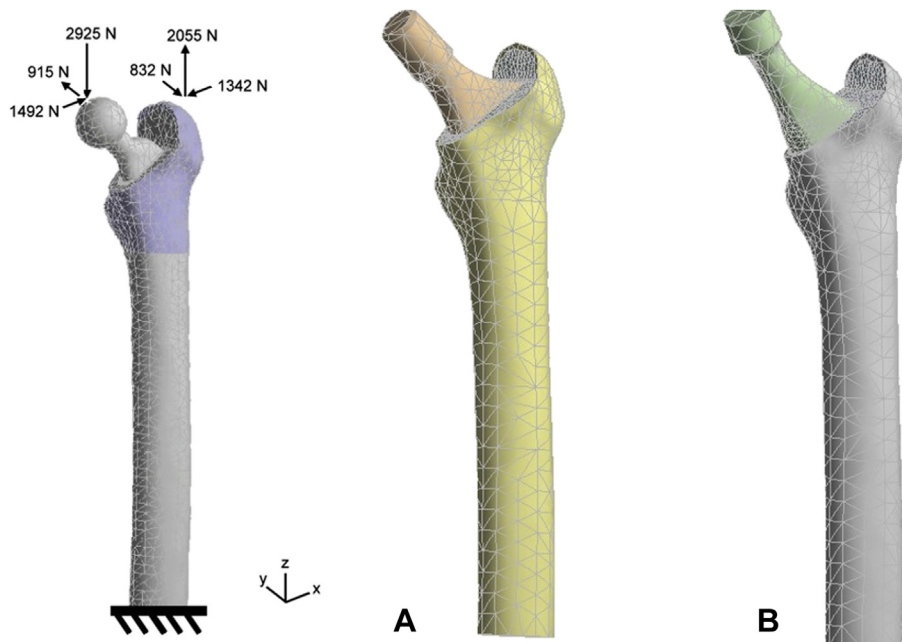


**Figure 2** The element mesh and loading conditions for the femoral bone and the cementless hip stem: (A)  $N_S$  model; (B)  $N_A$  model.  $N_A$  = anatomic femoral stem;  $N_S$  = straight femoral stem.

the body weight with force components:  $(x, y, z) = (-1342, -832, 2055)$  N] [14], as shown in Fig. 2. Both models were fully constrained at the distal ends of the cortex.

In order to simulate the initial condition of the bone/stem interface after stem insertion, the interface was prescribed as a Coulomb frictional interface, where a coefficient of friction of 0.3 was assigned [15]. For this purpose, the surface-to-surface contact elements were used, allowing contact, sliding, and tensile separation to occur. All solutions were processed using ANSYS 7.0 (ANSYS Inc., Canonsburg, PA, USA).

The stability of the stem was determined by the magnitude of micromotion between bone/stem interfaces in each contact element. A magnitude of micromotion under  $50 \mu\text{m}$  can be expected for bone ingrowth, from  $50 \mu\text{m}$  to  $150 \mu\text{m}$  as probable bone ingrowth, and greater than  $150 \mu\text{m}$  as non-bone ingrowth. The stem was divided into proximal, middle, and distal regions to adequately represent the biomechanical performance. The distribution of von Mises stress on the cortex was considered as an index of longterm stability of the stem. Lower stress than intact femur on the cortex would lead to a stress shielding effect and cause stem loosening.

## Results

The performance of micromotion between the bone/stem interface in models  $N_S$  and  $N_A$  is shown in Fig. 3. The results showed that relatively large micromotion occurred at the distal and posterior femur, whereas the largest was found at the lateral side of the distal femur. Relatively low von Mises stress occurred at the surface of the proximal femur. Fig. 4A illustrates the distribution of the von Mises stress on the medial and lateral femur in intact,  $N_S$ , and  $N_A$  models.

The geometrical effect of the femoral stem under various stiffness assignments of cancellous bone on the micromotion of the femoral stem in  $N_S$  and  $N_A$  models is shown in Table 1. When the hip joint (with 100% cancellous bone stiffness) is in the loading condition of heel strike (during a gait cycle), the peak micromotion between the bone and the femoral stem is  $124.35 \mu\text{m}$ , whereas the micromotion of 39.3% of the contact surface was over  $50 \mu\text{m}$  and 0% was over  $150 \mu\text{m}$  after implantation of a straight femoral stem ( $N_S$  model); however, if the anatomic stem ( $N_A$  model) was implanted instead, the peak micromotion between bone/stem interface was  $203.62 \mu\text{m}$ , whereas the micromotion of 38.97% of the contact surface was over  $50 \mu\text{m}$  and 2.2% was over  $150 \mu\text{m}$  (Table 1). By observing the distribution of micromotion at the proximal region of stem, the micromotion of the  $N_A$  model ( $112.49 \mu\text{m}$ ) was lower than the  $N_S$  model ( $119.35 \mu\text{m}$ ; Table 2). By contrast, by observing the distribution of micromotion at the distal region of the stem, the micromotion of the  $N_A$  model ( $203.62 \mu\text{m}$ ) was larger than the  $N_S$  model ( $124.35 \mu\text{m}$ ; Table 3).

When the stiffness of femoral cancellous bone was decreased from 100% to 50% (simulating AVN) in the  $N_S$  model, the peak micromotion between bone/stem interface was increased to  $175 \mu\text{m}$ , the percentage of micromotion of the contact surface over  $50 \mu\text{m}$  was increased to 52%, and micromotion over  $150 \mu\text{m}$  was also increased to 0.69%. By contrast, in the  $N_A$  model, the peak micromotion between the bone/stem interface was increased to  $229.62 \mu\text{m}$ , the percentage of micromotion of the contact surface over  $50 \mu\text{m}$  was increased to 50.9%, and micromotion over  $150 \mu\text{m}$  was also increased to 4.3% (Table 1).

The relationship between von Mises stress and the location of the femoral cortex is shown in Fig. 4A. The distributions of von Mises stress at the proximal femur in both  $N_A$  and  $N_S$  models were similar. Moreover, the von

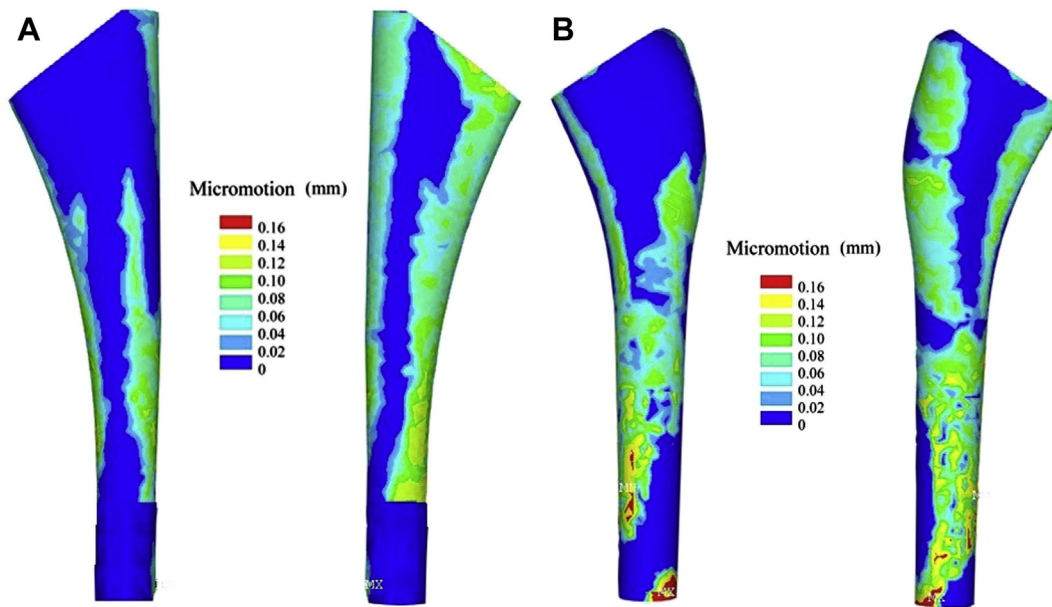


**Figure 3** Micromotion between the bone/stem interface in (A) the  $N_S$  model and (B) the  $N_A$  model. Left: anterior contact surface; right: posterior contact surface.  $N_A$  = anatomic femoral stem;  $N_S$  = straight femoral stem.

Mises stress at the location 20 mm proximal to the end of the femur was around 10 MPa larger in the  $N_A$  model than that in the  $N_S$  model; in the  $N_S$  model, the von Mises stress at the location 60 mm proximal to the end of the femur was around 12 MPa larger than that in the  $N_A$  model; the von Mises stress at the location 100 mm proximal to the end of the femur was around 7 MPa larger in the  $N_A$  model than that in the  $N_S$  model.

There was no noticeable change in the distribution of von Mises stress found at the proximal femur with the decrease of cancellous bone stiffness by 50%. As reflected, the decrease in stiffness of the femoral cancellous bone did not remarkably alter the stress shielding effect of the femoral stem (Fig. 4B and C).

## Discussion

Many finite element studies have reported various findings on the topic of cementless THR, but none of them has ever investigated the problem of the effects of metaphysis stiffness and stem geometry on AVN patients after THR. Although finite element modelling is relatively easy, the limitations of this study still exist. The material properties of the bone and implant were assumed to be isotropic, linearly elastic, and homogeneous. In practice, simply tilting the stem could influence the results and, hence, performances in stress distribution and micromotion would be different. In the current study, we assumed that all stems were centralized in the canal.

When discussing the magnitude of micromotion between contact surfaces in  $N_S$  and  $N_A$  models, many previous studies have applied the distribution of micromotion and the peak micromotion as criteria for comparison, but could not provide sufficient information to exactly identify the influence on bone ingrowth. This study used not only

distribution and peak value of micromotion, but considered the percentage of the micromotion on the specific contact surface area for detailed comparison between the two models. The concept of this method was adopted and modified from the stress/volume method of Lennon and Prendergast [16]. In this study, we calculated the percentage of nodes where micromotion was over 50  $\mu\text{m}$  or over 150  $\mu\text{m}$  among all of the nodes located at the bone/stem contact interface. This index is capable of revealing that possible bone ingrowth onto the femoral stem may take place once the calculated magnitude of micromotion is under the growth-inducing threshold of the bone. If the peak values of micromotion are extremely close, this method may provide additional information for further comparison and evaluation.

Cementless femoral stems are generally provided for young patients or patients with good bone quality, indicating that the general geometry of the femoral canal in this population can be categorized as normal or champagne-flute type (canal flare index  $\geq 3$ ). However, young patients with nontraumatic osteonecrosis of the femoral head have weaker cancellous bone than normal subjects at the proximal femur. Arlot et al. [8] found that the aseptic loosening rate of the femoral stem in nontraumatic AVN patients after THR was higher than in patients who had traumatic AVN. Yet, related research on the femoral stem stability of nontraumatic AVN patient is rarely reported. The current study has simulated traumatic (normal stiffness of the cancellous bone) and nontraumatic (decreased stiffness of the cancellous bone) AVN by using finite element models. Referring to our results, decreased stiffness of the cancellous bone would cause increased micromotion at the contact surface between the bone/stem interface, representing a higher risk of instability of the femoral stem. Diaphysis fixation is the basic rationale to stabilize the straight stem in the femoral canal. In other

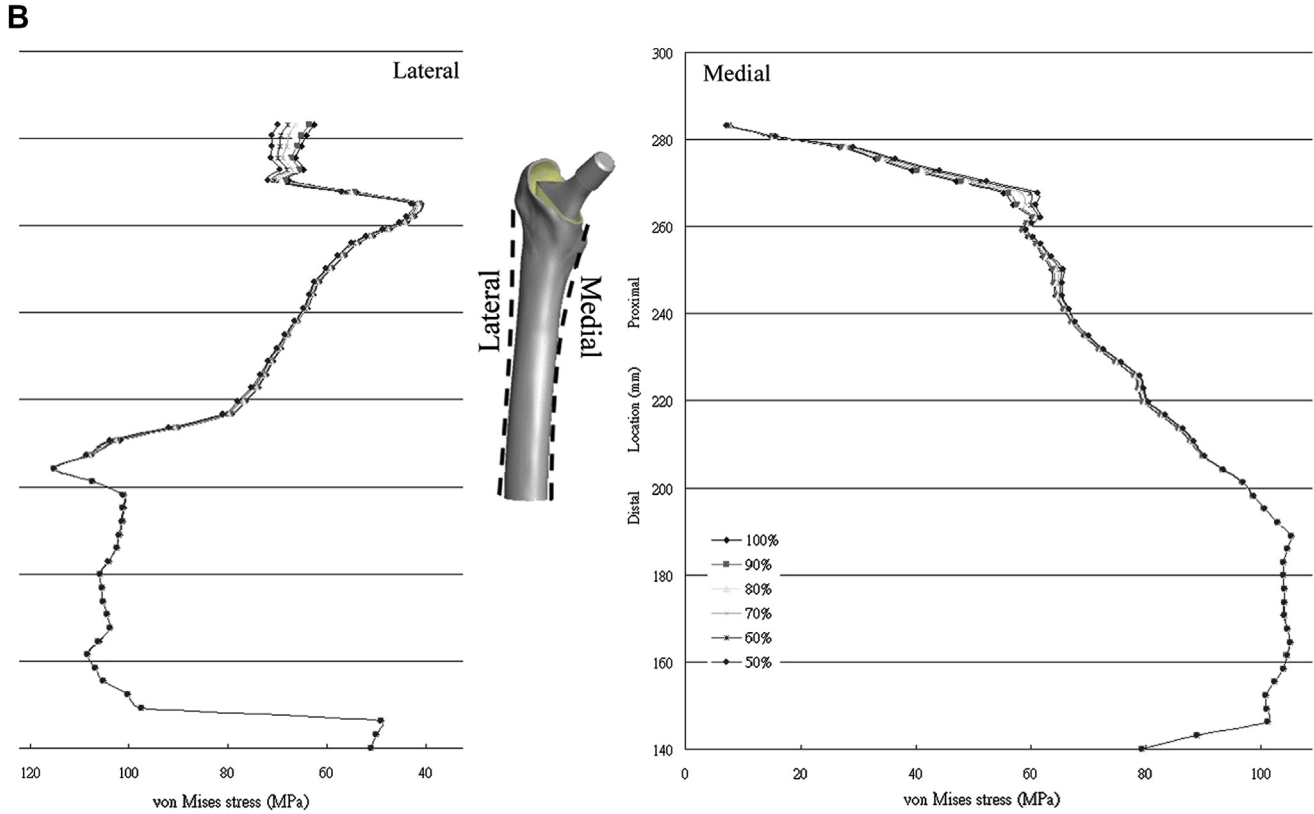
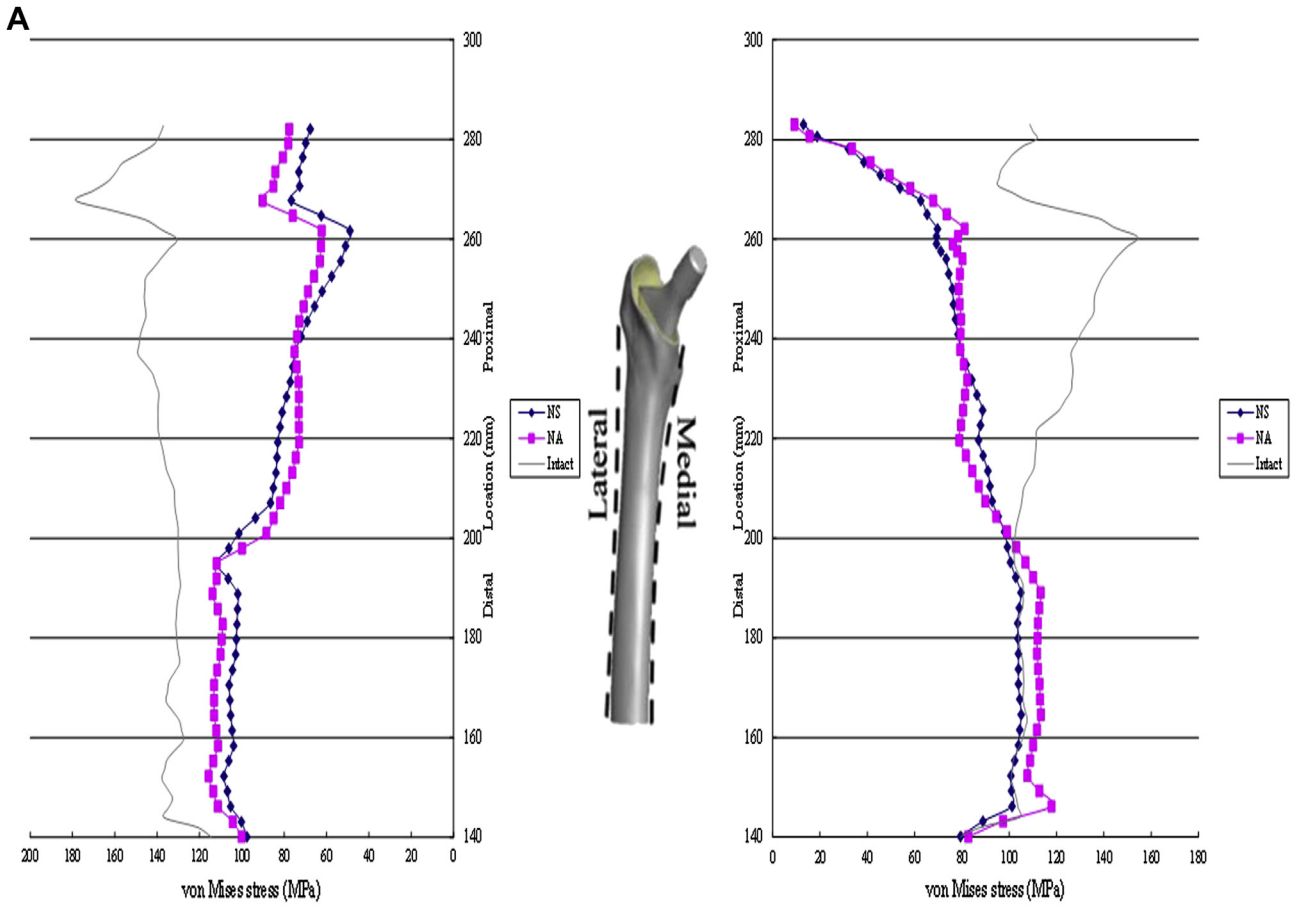


**Figure 4** (A) The distribution of von Mises stress at the medial and lateral femur in intact,  $N_S$ , and  $N_A$  models. (B) The influence of cancellous bone stiffness on von Mises stress located on the lateral (right) and medial (left) surfaces of the femoral cortex in the  $N_S$  model. (C) The influence of cancellous bone stiffness on von Mises stress located at the lateral (right) and medial (left) surfaces of the femoral cortex in the  $N_A$  model.  $N_A$  = anatomic femoral stem;  $N_S$  = straight femoral stem.

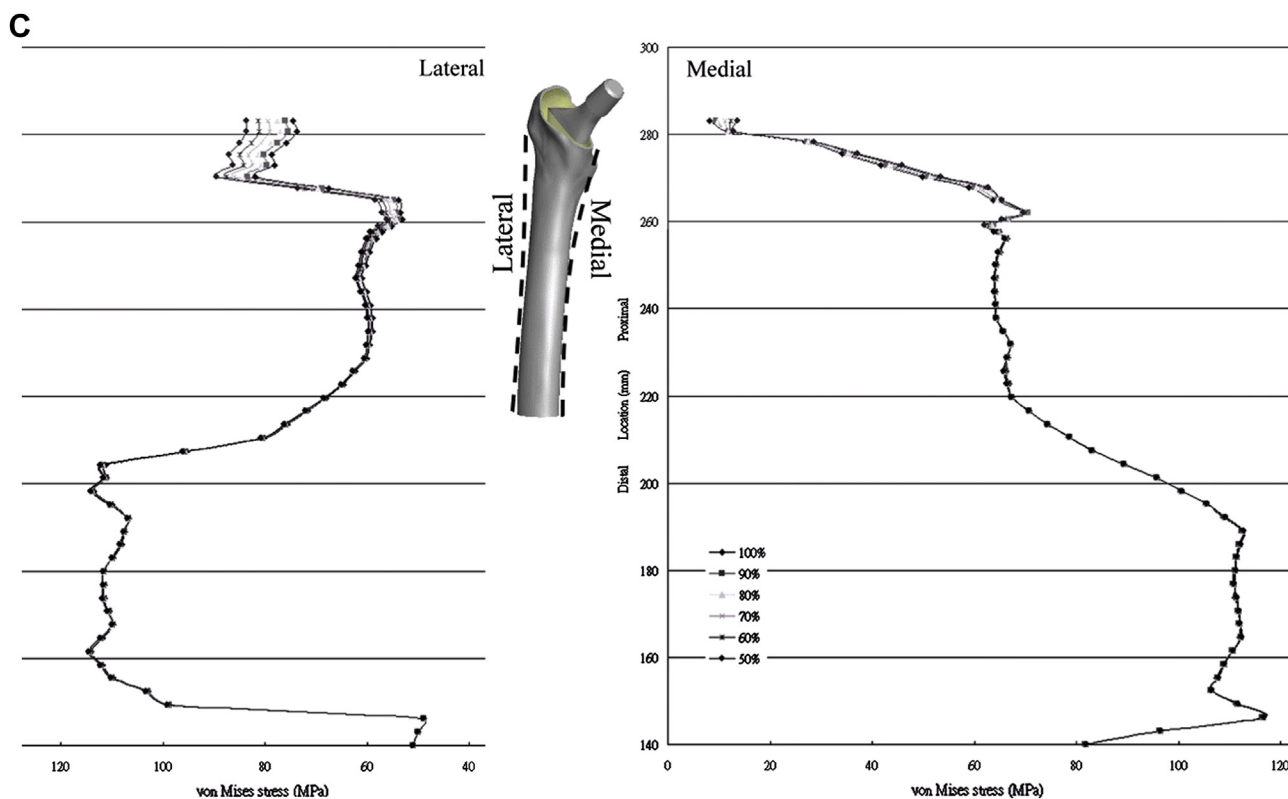


Figure 4 (continued).

words, the femoral stem size is determined by the dimension of the distal isthmus. Nevertheless, when the femoral stem is implanted into the femoral canal, a certain thickness of the cancellous bone must be kept in order to allow bone ingrowth onto the surface of the femoral stem. Therefore, poor quality of cancellous bone at the proximal femur would be insufficient for load bearing and result in a high magnitude of micromotion of the femoral stem [17].

The femoral rasp is applied to expand the canal prior to when the straight femoral stem is press-fitted with the geometries of the femoral canal and the isthmus. On the contrary, the purpose of the anatomic stem is to adjust the femoral stem to fit the geometry of the canal at the

proximal femur. Compared with the straight stem, the anatomic stem fills the metaphysis to achieve stabilization rather than diaphysis fitting [9]. Callaghan et al. [9] reported that no significant difference in micromotion was found between models implanted with anatomic and straight stems (peak value  $61\ \mu\text{m}$ ) under 1500 N at the simulated stance phase. However, our results showed that the peak micromotion was  $199.25\ \mu\text{m}$ , and the percentage of micromotion was over  $150\ \mu\text{m}$  (2.2%) in the  $N_A$  model, which was higher than that of the  $N_S$  model ( $135.7\ \mu\text{m}$ , 0%). The higher micromotion in the current study was the result of the larger loading (4.5 times the body weight) that was exerted in our finite element simulation than in the study of

Table 1 The performance of interfacial micromotion according to stiffness of cancellous bone.

|   | Stiffness of cancellous bone |        |        |        |        |        |
|---|------------------------------|--------|--------|--------|--------|--------|
|   | 100%                         | 90%    | 80%    | 70%    | 60%    | 50%    |
| $N_S$                                   |                              |        |        |        |        |        |
| % Contact surface $>50\ \mu\text{m}^a$  | 39.3                         | 42.5   | 45.1   | 47.3   | 49.6   | 52     |
| % Contact surface $>150\ \mu\text{m}^b$ | 0                            | 0      | 0      | 0      | 0.09   | 0.69   |
| Peak micromotion ( $\mu\text{m}$ )      | 124.35                       | 128.23 | 134.37 | 144.58 | 157.44 | 175    |
| $N_A$                                   |                              |        |        |        |        |        |
| % Contact surface $>50\ \mu\text{m}^a$  | 38.97                        | 41.2   | 42.2   | 45.6   | 48     | 50.9   |
| % Contact surface $>150\ \mu\text{m}^b$ | 2.2                          | 2.3    | 2.9    | 3      | 3.4    | 4.3    |
| Peak micromotion ( $\mu\text{m}$ )      | 203.62                       | 206.74 | 207.36 | 216.24 | 221.85 | 229.26 |

$N_A$  = anatomic femoral stem;  $N_S$  = straight femoral stem.

<sup>a</sup> % Contact surface  $>50\ \mu\text{m}$  = percentage of the micromotion of the contact surface of bone and femoral stem over  $50\ \mu\text{m}$ .

<sup>b</sup> % Contact surface  $>150\ \mu\text{m}$  = percentage of the micromotion of the contact surface of bone and femoral stem over  $150\ \mu\text{m}$ .

**Table 2** The performance of interfacial micromotion at the proximal region of the femoral stem according to stiffness of cancellous bone.

|  | Stiffness of cancellous bone |       |        |        |        |        |
|--|------------------------------|-------|--------|--------|--------|--------|
|  | 100%                         | 90%   | 80%    | 70%    | 60%    | 50%    |
| $N_S$                                  |                              |       |        |        |        |        |
| % Contact surface $>50 \mu\text{m}^a$  | 30.6                         | 34.5  | 37.7   | 40     | 42     | 44.4   |
| % Contact surface $>150 \mu\text{m}^b$ | 0                            | 0     | 0      | 0      | 0.2    | 1.36   |
| Peak micromotion ( $\mu\text{m}$ )     | 119.35                       | 126.2 | 134.37 | 144.58 | 157.44 | 175    |
| $N_A$                                  |                              |       |        |        |        |        |
| % Contact surface $>50 \mu\text{m}^a$  | 31.5                         | 33.2  | 34.15  | 37     | 39.3   | 42.1   |
| % Contact surface $>150 \mu\text{m}^b$ | 0                            | 0     | 0      | 0      | 0      | 0      |
| Peak micromotion ( $\mu\text{m}$ )     | 112.49                       | 113.8 | 115.78 | 126.55 | 134.23 | 148.28 |

$N_A$  = anatomic femoral stem;  $N_S$  = straight femoral stem.

<sup>a</sup> % Contact surface  $>50 \mu\text{m}$  = percentage of the micromotion of the contact surface of bone and femoral stem over  $50 \mu\text{m}$ .

<sup>b</sup> % Contact surface  $>150 \mu\text{m}$  = percentage of the micromotion of the contact surface of bone and femoral stem over  $150 \mu\text{m}$ .

Callaghan et al. [9] (2.4 times the body weight). The reduced stiffness of cancellous bone at the metaphysis due to AVN can hardly bear the load; this is represented in the higher micromotion (peak value of  $225.68 \mu\text{m}$ ) and poor bone ingrowth (4.27% of micromotion over  $150 \mu\text{m}$ ) in the  $N_A$  model than in the  $N_S$  model. According to these results, the anatomic stem is not recommended for patients with weak cancellous bone.

Decking et al. [18] measured the strain on the surface of the femoral cortex for evaluating the stress shielding effect after implantation of traditional straight and anatomic stems, and no statistical differences were found. Similar results were observed in the current study. Moreover, our results showed that the changes in stiffness of cancellous bone did not obviously influence stress transition (Fig. 4B and C). As for local performance in the stress response, higher stress was found in the  $N_A$  model in the proximal femoral area (proximal femur at 20 mm) than in the  $N_S$  model. By contrast, the stress of the  $N_S$  model is higher than that of the  $N_A$  model in the distal region of the stem. Compared with the simulated results for micromotion at the bone/stem interface, the stress shielding effect may not be the major factor that causes stem loosening in AVN patients after THR.

Because the curvature of the stem is considered in the design of the anatomic stem, the length of the anatomic stem will be shorter than the straight one for the same size product. The anterior and posterior aspects of the proximal femoral canal are both curvature contours. If the length of the anatomic stem is too long, the distal stem and the canal will collide with each other and get stuck at the proximal femur during implantation. Keaveny and Bartel [19] considered that if the femoral stem has a high frictional coefficient and large contact surface, the micromotion of the femoral stem at the initial stage can be reduced. With identical geometry of the femoral stem, if the femoral stem shows bone ingrowth, the micromotion of the longer femoral stem would also be decreased, but the stress shielding effect would be relatively higher at the proximal femur. In the current study, the larger micromotion in the  $N_A$  model than that in the  $N_S$  model at the distal femur may be due to the shorter length of the anatomic stem than the straight stem. Comparable results have been revealed in the study of Laine et al. [20] where the straight stem had greater conformity at the diaphysis than that of the anatomic stem, which becomes one of the reasons why the subsidence of the stem can be lower after surgery.

**Table 3** The performance of interfacial micromotion at the distal region of the femoral stem according to stiffness of cancellous bone.

|  | Stiffness of cancellous bone |        |        |        |        |        |
|--|------------------------------|--------|--------|--------|--------|--------|
|  | 100%                         | 90%    | 80%    | 70%    | 60%    | 50%    |
| $N_S$                                  |                              |        |        |        |        |        |
| % Contact surface $>50 \mu\text{m}^a$  | 46.6                         | 47.7   | 48.4   | 49.7   | 51.4   | 52.8   |
| % Contact surface $>150 \mu\text{m}^b$ | 0                            | 0      | 0      | 0      | 0      | 0.11   |
| Peak micromotion ( $\mu\text{m}$ )     | 124.35                       | 128.23 | 132.8  | 138.33 | 145.23 | 154.24 |
| $N_A$                                  |                              |        |        |        |        |        |
| % Contact surface $>50 \mu\text{m}^a$  | 43.5                         | 44.8   | 46     | 47.8   | 49.6   | 51.2   |
| % Contact surface $>150 \mu\text{m}^b$ | 6.1                          | 6.5    | 8      | 8.16   | 9.29   | 11     |
| Peak micromotion ( $\mu\text{m}$ )     | 203.62                       | 206.74 | 207.36 | 216.24 | 221.85 | 229.26 |

$N_A$  = anatomic femoral stem;  $N_S$  = straight femoral stem.

<sup>a</sup> % Contact surface  $>50 \mu\text{m}$  = percentage of the micromotion of the contact surface of bone and femoral stem over  $50 \mu\text{m}$ .

<sup>b</sup> % Contact surface  $>150 \mu\text{m}$  = percentage of the micromotion of the contact surface of bone and femoral stem over  $150 \mu\text{m}$ .

In conclusion, stiffness of cancellous bone at the metaphysis in patients with nontraumatic AVN of the femoral head should be carefully considered prior to selecting a femoral stem in hip replacement surgery. The poor bone quality of nontraumatic AVN patients may result in larger micromotion after cementless THR. Therefore, a cementless, straight stem that fills the isthmus would be a better choice than an anatomic stem that is fixed at the proximal part of the canal only.

### Conflicts of interest

All authors declare no conflicts of interest.

### Acknowledgements

We acknowledge funding support from the National Science Council Taiwan (NSC 99-2320-B-010-002) and the Southern Taiwan Science Park (BY-03-04-17-98).

### References

- [1] Lai YS, Wei HW, Cheng CK. Incidence of hip replacement among National Health Insurance enrollees in Taiwan. *J Orthop Surg Res* 2008;3:42.
- [2] Chiu KY, Ng TP, Tang WM, Yip D. Charnely total hip arthroplasty in Chinese patients less than 40 years old. *J Arthroplasty* 2001;16:92–101.
- [3] Jacobs B. Alcoholism-induced bone necrosis. *NY State J Med* 1992;92:334–8.
- [4] Abeles M, Urman JD, Rothfield NF. Aseptic necrosis of bone in systemic lupus erythematosus: relationship to corticosteroid therapy. *Arch Intern Med* 1978;138:750–4.
- [5] Cruess RL. Steroid-induced osteonecrosis. *JR Coll Surg Edinb* 1981;26:69–77.
- [6] Mont MA, Hungerford DS. Non-traumatic avascular necrosis of the femoral head. *J Bone Joint Surg Am* 1995;77:459–74.
- [7] Radl R, Egner S, Hungerford M, Rehak P, Windhager R. Survival of cementless femoral components after osteonecrosis of the femoral head with different etiologies. *J Arthroplasty* 2005;20:509–15.
- [8] Arlot ME, Bonjean M, Chavassieux PM, Meunier PJ. Bone histology in adults with aseptic necrosis. Histomorphometric evaluation of iliac biopsies in seventy-seven patients. *J Bone Joint Surg Am* 1983;65:1319–27.
- [9] Callaghan JJ, Fulghum CS, Glisson RR, Stranne SK. The effect of femoral stem geometry on interface motion in uncemented porous-coated total hip prostheses. Comparison of straight-stem and curved-stem designs. *J Bone Joint Surg Am* 1992;74:839–48.
- [10] Szmukler-Moncler S, Salama H, Reingewirtz Y, Dubrille JH. Timing of loading and effect of micromotion on bone-dental implant interface: review of experimental literature. *J Biomed Mater Res* 1998;43:192–203.
- [11] Ramamurti BS, Orr TE, Bragdon CR, Lowenstein JD, Jasty M, Harris WH. Factors influencing stability at the interface between a porous surface and cancellous bone: a finite element analysis of a canine *in vivo* micromotion experiment. *J Biomed Mater Res* 1997;36:274–80.
- [12] Lai YS, Wei HW, Chang TK, Cheng CK. The effects of femoral canal geometries, stem shapes, cement thickness, and stem materials on the choice of femoral implant in cemented total hip replacement. *J Chin Inst Eng* 2009;32:333–41.
- [13] Mann KA, Bartel DL, Wright TM, Burstein AH. Coulomb frictional interfaces in modeling cemented total hip replacements: a more realistic model. *J Biomech* 1995;28:1067–78.
- [14] Verdonschot N, Huiskes R. Acrylic cement creeps but does not allow much subsidence of femoral stems. *J Bone Joint Surg Br* 1997;79:665–9.
- [15] Viceconti M, Muccini R, Bernakiewicz M, Baleani M, Cristofolini L. Large-sliding contact elements accurately predict levels of bone–implant micromotion relevant to osseointegration. *J Biomech* 2000;33:1611–8.
- [16] Lennon AB, Prendergast PJ. Evaluation of cement stresses in finite element analyses of cemented orthopaedic implants. *Trans ASME J Biomech Eng* 2001;123:623–8.
- [17] Okano T, Hagino H, Otsuka T, Teshima R, Yamamoto K, Hirano Y, et al. Measurement of periprosthetic bone mineral density by dual-energy X-ray absorptiometry is useful for estimating fixation between the bone and the prosthesis in an early stage. *J Arthroplasty* 2002;17:49–55.
- [18] Decking R, Puhl W, Simon U, Claes LE. Changes in strain distribution of loaded proximal femora caused by different types of cementless femoral stems. *Clin Biomech* 2006;21:495–501.
- [19] Keaveny TM, Bartel DL. Effects of porous coating, with and without collar support, on early relative motion for a cementless hip prosthesis. *J Biomech* 1993;26:1355–68.
- [20] Laine HJ, Puolakka TJS, Moilanen T, Pajamäki KJ, Wirta J, Lehto MUK. The effects of cementless femoral stem shape and proximal surface texture on “fit-and-fill” characteristics and on bone remodelling. *Int Orthop* 2000;24:184–90.